Research in
Astronomy and
Astrophysics

A statistical classification of the unassociated gamma-ray sources in the second Fermi Large Area Telescope Catalog *

Zhu Mao and Yun-Wei Yu

Institute of Astrophysics, Central China Normal University, Wuhan 430079, China;
yuyw@phy.ccnu.edu.cn

Abstract With the assistance of the identified/associated sources in the second Fermi Large Area Telescope (LAT) catalog, we analyze and resolve the spatial distribution and the distributions of the gamma-ray spectral and variability indices of the remaining 575 unassociated Fermi LAT sources. Consequently, it is suggested that the unassociated sources could statistically consist of Galactic supernova remnants/pulsar wind nebulae, BL Lacertae objects, flat spectrum radio quasars and other types of active galaxies with fractions of 25%, 29%, 41% and 5%, respectively.

Key words: gamma rays: general — catalogs — methods: statistical

1 INTRODUCTION

A routine whole-sky survey in the 100 MeV to 100 GeV band with the Large Area Telescope (LAT; Atwood et al. 2009) onboard the *Fermi Gamma-Ray Space Telescope* has been carried out since the science phase of the mission began in August 2008. By analyzing the observational results of the first 24 months, the Fermi LAT Collaboration published the second Fermi LAT Source Catalog containing 1873 gamma-ray sources (Nolan et al. 2012). Great efforts have been made to identify the LAT sources by periodic emission or variability correlation with other wavelengths, and also to provide associations for many more LAT sources with previous gamma-ray catalogs and with likely counterpart sources from known or suspected source classes (based on Bayesian probabilities in a LAT error box). As a result, 1298 LAT sources have been identified as or associated with pulsars, supernova remnants (SNRs), pulsar wind nebulae (PWNe), blazars, active galaxies (AGs), etc (see Table 1). However, nearly one third of the LAT sources are still unclassified (i.e. 575 out of 1873). Such a situation is similar to that of the third *Energetic Gamma Ray Experiment Telescope* (EGRET) catalog (Hartman et al. 1999).

The difficulty in the identification/association of these unclassified sources arises because of the location accuracy of the LAT sources, which is typically insufficiently precise. In other words, in a typical LAT error box, there are too many stars, galaxies, X-ray sources, infrared sources and radio sources. Therefore, besides the source positions, more information is required to determine the nature of the unassociated LAT sources, including the spectral information, time variability, and availability of a plausible physical process at the source to produce gamma-rays with sufficiently-high energy. Stephen et al. (2010) made such an attempt with the *ROSAT* catalog, which is useful

Table 1 The Numbers of Identified/Associated Sources in the Second Fermi LAT Catalog

Type	No.
Pulsar	108
Pulsar wind nebula	3
Supernova remnant	10
Supernova remnant/Pulsar wind nebula	58
Globular cluster	11
High-mass binary	4
Nova	1
BL Lacerate object	436
Flat spectrum radio quasar	370
Active galaxy with an uncertain type	257
Non-blazar active galaxy	11
Radio galaxy	12
Seyfert galaxy	6
Normal galaxy	6
Starburst galaxy	4

in finding a positionally corrected, highly unusual object that might be expected to produce gamma-rays. As a result, 30 unassociated LAT sources are tentatively suggested to be associated with a *ROSAT* counterpart. More directly, Ferrara et al. (2012) proposed that a comparison of the spectral and variability indices between the associated and unassociated LAT sources can provide insight into the likely classes of the unassociated sources. Following such a consideration, in this paper, we provide statistics on the gamma-ray spectral and variability indices of the unassociated Fermi LAT sources. Based on these statistics, we try to discover how many components the unassociated sources consist of and what these components could be.

2 SKY DISTRIBUTION OF THE UNASSOCIATED FERMI LAT SOURCES

The spatial distribution of the 575 unassociated Fermi LAT sources is presented in the left panel of Figure 1, which exhibits an obvious concentration of the sources in the galactic plane (GP). In more detail, we show the latitude distribution of these sources in the right panel of Figure 1, where a spike in the source number appears in the central $\sim 10°$ of the Galaxy. Such a spike naturally indicates a Galactic origin for a significant fraction of the unassociated sources. However, it should be noted that the spike could also be partly contributed by some active galactic nuclei (AGNs) because of the anisotropic distribution of the identified/associated AGNs.

As shown in Figure 2, a big dip appears in the AGN number distribution, which is caused by the limited/no coverage of the AGN catalogs in the GP (Ackermann et al. 2012). Therefore, by considering the actual isotropic distribution of AGNs, an extra component consisting of potential AGNs is expected to exist in the unassociated sources. According to the fitting to the latitude distribution of all identified/associated AGNs in Figure 2, the number density of the potential AGNs per square degree as a function of galactic latitude can be empirically described by the following Gaussian function

$$n_{\text{pAGN}}(b) = n_{\text{pAGN,max}} e^{-(b-\mu_b)^2/2\sigma_b^2} \tag{1}$$

with $n_{\text{pAGN,max}} = 0.02 \text{ deg}^{-2}$, $\mu_b = -1.6°$ and $\sigma_b = 6.5°$. Besides these potential AGNs, the unassociated sources could still contain an isotropically-distributed (ISO) component and a GP component. For a simple empirical description, we express the number densities of the ISO and GP components by a constant and a Gaussian function, respectively. Then, as shown in the right panel of
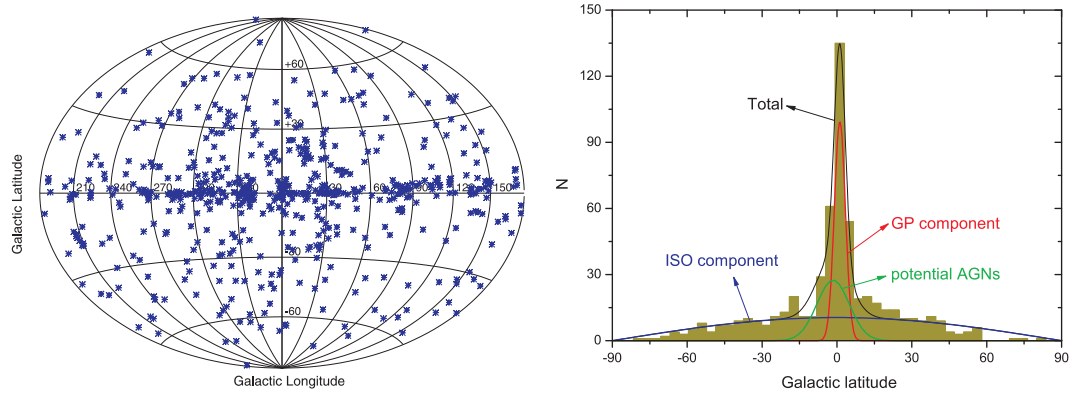
Fig. 1 *Left*: the spatial distribution of the 575 unassociated sources in galactic coordinates. *Right*: the latitude distribution of all unassociated sources and an empirical fitting to the distribution with three components as labeled.
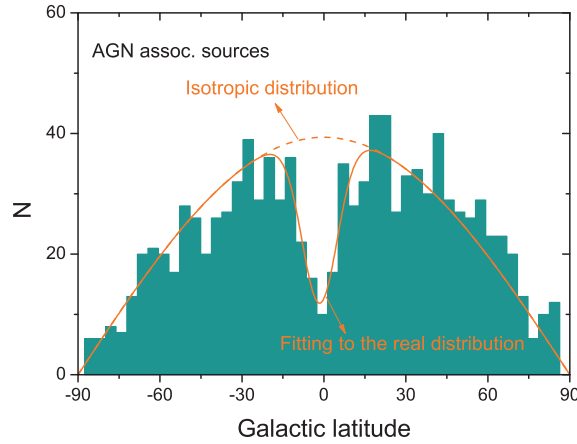
Fig. 2 The latitude distribution of the sources associated with AGNs, which is empirically fitted by the solid line. The dashed line exhibits an isotropic distribution for comparison.

Figure 1, the numbers of unassociated sources within each $4°$ bin as a function of latitude can be fitted by the following function

$$N_{\text{bin}}(b) = \left[n_{\text{GP,max}} e^{-(b-\mu_b)^2/2\sigma_b^2} + n_{\text{ISO}} + n_{\text{pAGN}}(b) \right] (2\pi \cos b \Delta b) \qquad (2)$$

with $n_{\text{GP,max}} = 0.07 \deg^{-2}$, $\mu_b = 1.2°$, $\sigma_b = 2.2°$ and $n_{\text{ISO}} = 0.007 \deg^{-2}$, where the factor $2\pi \cos b \Delta b$ represents the sky area of each latitude bin.

Equation (2) indicates that the unassociated Fermi LAT sources can be statistically separated into three components including the GP, ISO and potential AGN components, the fractions of which are about $f_{\text{GP}} = 25\%$, $f_{\text{ISO}} = 55\%$ and $f_{\text{pAGN}} = 20\%$, respectively. The fractions are obtained by integrating the densities over the whole sky. Roughly speaking, one quarter of the unassociated

Table 2 Fitting Parameters for Distributions of Γ and V

	Γ		$\log V$	
	μ	σ	μ	σ
ISO-I	2.075	0.204	1.345	0.187
ISO-II	2.451	0.174	1.380	0.073
GP	2.440	0.207	1.364	0.132

sources have Galactic origins, while the other three quarters are possible extragalactic sources. Of course, such a conclusion can be somewhat modified by some pulsars and some possible exotic sources (e.g. due to dark matter annihilation (Zechlin & Horns 2012)), which could be located in the Galactic halo and contribute to the ISO component.

3 POSSIBLE NATURES OF THE UNASSOCIATED FERMI LAT SOURCES

As provided by the Fermi LAT collaboration (Abdo et al. 2010; Nolan et al. 2012), the gamma-ray properties of the unassociated sources can be characterized by four basic parameters of flux S, time variability index V, spectral index Γ and curvature index C, which quantifies the departure of the spectrum from a single power-law shape. In this paper, we make a basic assumption that a quantity which reflects an intrinsic physical property of a source type should exhibit a normal or lognormal distribution. However, due to the distance-dependence of S and the possible flux-dependence of C (Ackermann et al. 2012), these two parameters are not considered to be good statistical quantities. Therefore, we will only include the spectral and variability indices, Γ and V, in our work.

3.1 The ISO Component

In order to reveal the possible nature of the ISO component, we select the unassociated sources at latitudes higher than $|b| = 18°$, the number of which is $N_{\mathrm{HL}} = 205$. According to the fitting given in the right panel of Figure 1, it is certain that all of these 205 high-latitude (HL) sources are part of the ISO component.

In Figure 3, we display the number distributions of the spectral and variability indices of the 205 HL/ISO unassociated sources by histograms. What do these distributions tell us? Following our basic assumption, the distributions of Γ and V are fitted simultaneously and tentatively by one, two or three Gaussians. By comparison, the best fit is obtained with two Gaussians, as shown in Figure 3. The fitting function reads

$$N_{\mathrm{bin}} = \frac{\mathcal{R}A}{\sigma_{\mathrm{I}}\sqrt{2\pi}}e^{-(b-\mu_{\mathrm{I}})^2/2\sigma_{\mathrm{I}}^2} + \frac{A}{\sigma_{\mathrm{II}}\sqrt{2\pi}}e^{-(b-\mu_{\mathrm{II}})^2/2\sigma_{\mathrm{II}}^2}, \tag{3}$$

and the fitting parameters are listed in Table 2 for $\mathcal{R} = 1.5$. Here we would like to emphasize that the ratio $\mathcal{R}$ between the numbers of the two Gaussian components should be the same in both the Γ and V fittings. According to the above fittings, we can further separate the ISO component into two subcomponents, denoted by ISO-I and ISO-II. Relative to the total unassociated sources, the percentages of the ISO-I and ISO-II components can be estimated as $f_{\mathrm{ISO-I}} = f_{\mathrm{ISO}}\frac{\mathcal{R}}{1+\mathcal{R}} = 33\%$ and $f_{\mathrm{ISO-II}} = f_{\mathrm{ISO}}\frac{1}{1+\mathcal{R}} = 22\%$, respectively.

In the left panel of Figure 4, we draw a scatter plot for the 205 HL/ISO unassociated sources in the $\Gamma - V$ plane and show the 2σ regions of the ISO-I and ISO-II components by the rectangles defined by Equation (3). As can be seen, most of the data are covered by the two rectangles, except for the data at the far left and the top right corner. In the right panel of Figure 4, nearly all of the
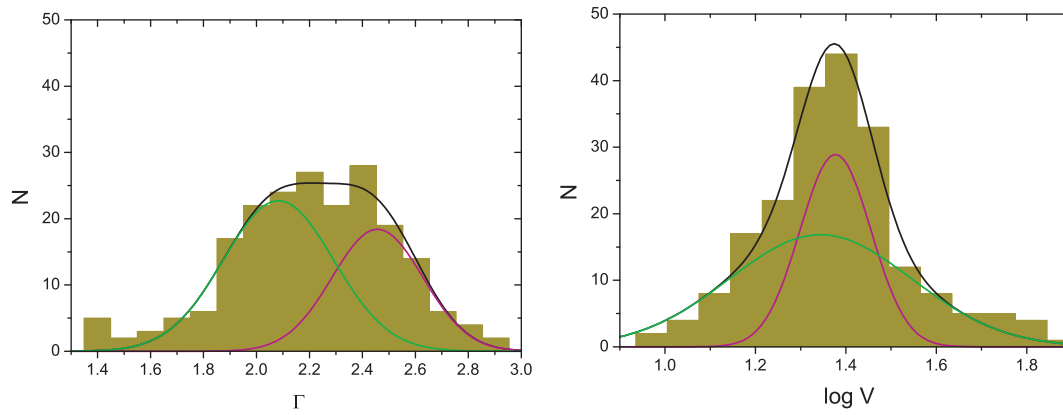
Fig. 3 The distributions of the spectral (*left*) and variability (*right*) indices of the 205 HL/ISO unassociated sources, both of which are fitted by the sum of two Gaussians.
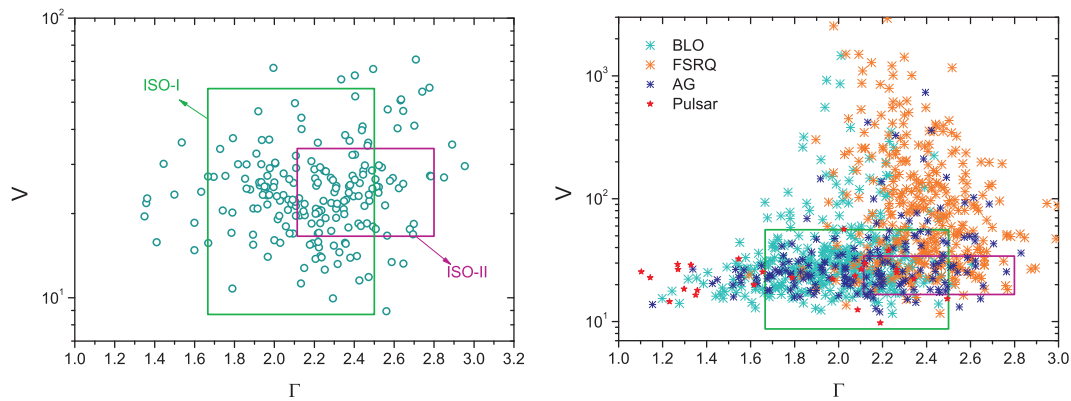
Fig. 4 *Left*: the $\Gamma - V$ distribution of the 205 HL/ISO unassociated sources, where the rectangles represent the 2σ regions of the ISO-I and ISO-II components. *Right*: a comparison between the 2σ regions of the ISO-I and ISO-II components with the identified/associated sources at $|b| \geq 18°$ including blazars, AGs and pulsars.

identified/associated sources at $|b| \geq 18°$, including BL Lacerate objects (BLOs), flat spectrum radio quasars (FSRQs), AGs [1], and pulsars, are displayed in comparison with the obtained 2σ regions of the HL/ISO unassociated sources, which show that: (i) all of the sources with a large variability are associated with AGNs, and the V-range of the unassociated sources basically overlaps with the region occupied by pulsars. (ii) The Γ-values of the HL/ISO unassociated sources are in good agreement with those of most AGNs, but are somewhat higher than pulsars. At the same time, the offset between the Γ-ranges of the BLOs and FSRQs is well reproduced by the ISO-I and ISO-II components. Therefore, we suggest that the classifications of the ISO-I and ISO-II unassociated sources could be BLOs and FSRQs, respectively. Finally, (iii) according to the distribution of pulsars, in principle, it cannot be ruled out that some sources classified as the ISO-I component are actually pulsars. However, the scarcity of unassociated sources with a hard spectrum, which should be usual

---

[1] From a statistical view, we treat all of the active galaxies that have uncertain type, non-blazar active galaxies, radio galaxies, Seyfert galaxies, starburst galaxies and normal galaxies with strong gamma-ray emission as active galaxies.

in pulsars, could indicate a low probability of pulsars for the unassociated sources. By ignoring the possibility of being a pulsar, the numbers of unassociated sources which are candidates of BLOs and FSRQs can be estimated to be

$$N_{\mathrm{BLO\ cand}} = N_{\mathrm{unassoc}}(f_{\mathrm{ISO-I}} + f_{\mathrm{pAGN}}f_{\mathrm{BLO}}) = 235, \tag{4}$$

$$N_{\mathrm{FSRQ\ cand}} = N_{\mathrm{unassoc}}(f_{\mathrm{ISO-II}} + f_{\mathrm{pAGN}}f_{\mathrm{FSRQ}}) = 165, \tag{5}$$

where $N_{\mathrm{unassoc}} = 575$, and the fractions $f_{\mathrm{BLO}} = 39\%$ and $f_{\mathrm{FSRQ}} = 34\%$ are obtained by counting the numbers of identified/associated AGNs. Additionally, the remaining sources in the potential AGNs could be AG candidates, the number of which is about

$$N_{\mathrm{AG\ cand}} = N_{\mathrm{unassoc}}f_{\mathrm{pAGN}}(1 - f_{\mathrm{BLO}} - f_{\mathrm{FSRQ}}) = 31. \tag{6}$$

3.2 The GP Component

As a similar treatment, we select the unassociated sources at latitudes lower than $|b| = 8°$, the number of which is $N_{\mathrm{LL}} = 288$. According to the fitting in the right panel of Figure 1, we know that the low-latitude (LL) sources could be dominated by the sources that have a Galactic origin.

In Figure 5, we firstly display the distributions of Γ and V for the 288 LL unassociated sources by the grey histograms. However, these distributions cannot directly reflect the intrinsic properties of the GP component, because a significant fraction of the LL sources are actually extragalactic sources. According to Equation (2), we can derive the percentages of the different components in the latitude range of $|b| \leq 8°$ as $f_{\mathrm{LL,GP}} = 52\%$, $f_{\mathrm{LL,ISO}} = 16\%$ and $f_{\mathrm{LL,pAGN}} = 32\%$. Therefore, the intrinsic distributions of Γ and V for the GP sources can be obtained by the following method

$$N_{\mathrm{GP,bin}} = N_{\mathrm{LL,bin}} - f_{\mathrm{ISO}}N_{\mathrm{ISO,bin}} - f_{\mathrm{pAGN}}N_{\mathrm{pAGN,bin}}, \tag{7}$$

where $N_{\mathrm{ISO,bin}}$ and $N_{\mathrm{pAGN,bin}}$ are the numbers of the ISO unassociated sources and potential AGNs in each Γ or $\log V$ bin. As a result, the corrected distributions of Γ and V with only the GP component are presented by the dark yellow histograms in Figure 5, where two single-Gaussian fittings are provided. The fitting parameters are also listed in Table 2.

In the left panel of Figure 6, we draw a scatter plot for the 288 LL unassociated sources in the $\Gamma - V$ plane, where the 2σ region of the GP component is presented by the rectangle. As can be seen, a remarkable number of data points are located beyond the rectangle, in particular, in the low-Γ range, which is classified as the ISO sources and potential AGNs. In the right panel of Figure 6, we compare the 2σ region of the GP component with the identified/assocated GP sources including pulsars, SNRs and PWNe. The comparison suggests that most of the unassociated GP sources are probably candidates of SNRs/PWNe, rather than the generally expected pulsars. The number of these GP sources is

$$N_{\mathrm{SN/PWN\ cand}} = N_{\mathrm{unassoc}}f_{\mathrm{GP}} = 144. \tag{8}$$

Additionally, the GP component may also contain some globular clusters, because most identified/associated globular clusters are located in the bottom-left corner of the 2σ region, although their number is not very large.

3.3 Identification Efficiency

In Figure 7 we present the identification efficiencies of BLOs, FSRQs, AGs, SNRs/PWNe and pulsars by comparing the numbers of identified/associated sources with unassociated ones, where the potential AGNs are not considered in order to avoid the complication in the GP.
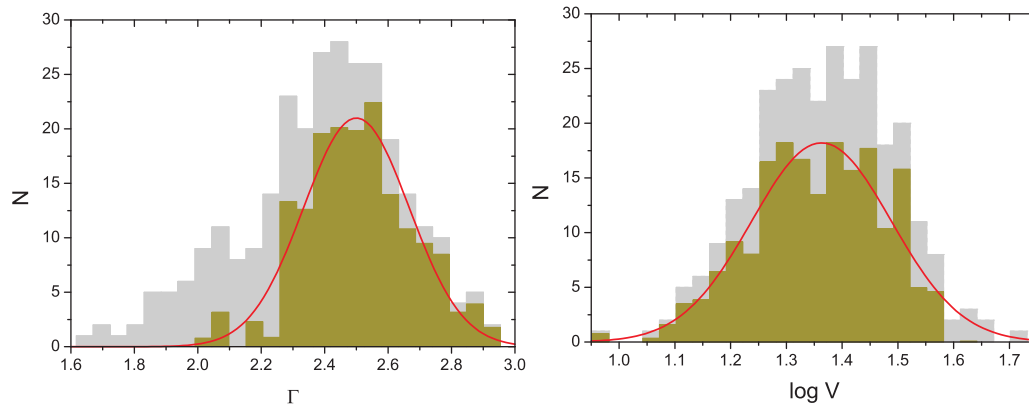
Fig. 5 The distributions of the spectral (*left*) and variability (*right*) indices of the 288 LL unasso-ciated sources (*grey histograms*) and the corrected distributions of only the GP component (*dark yellow histograms*). The solid lines provide a single Gaussian fitting to the GP sources.
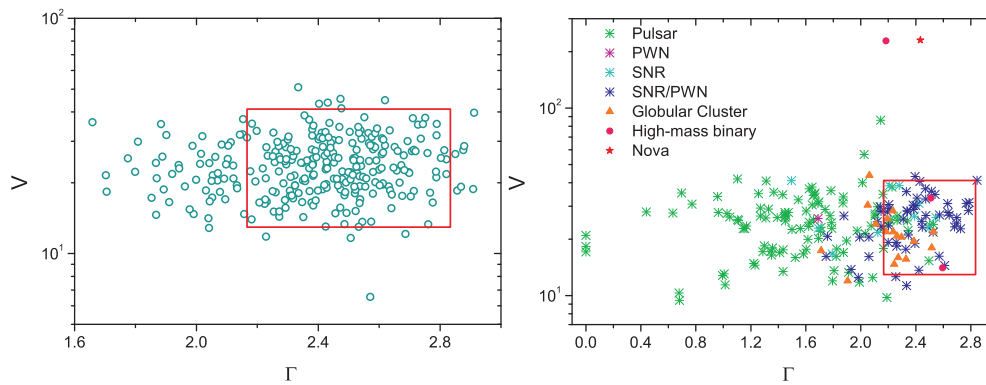
Fig. 6 *Left*: the $\Gamma - V$ distribution of the 288 LL unassociated sources, where the rectangle represents the 2σ regions of the GP component. *Right*: a comparison between the 2σ region of the GP compo-nent with the identified/associated sources that have a Galactic origin, including pulsars, SNRs and PWNe.
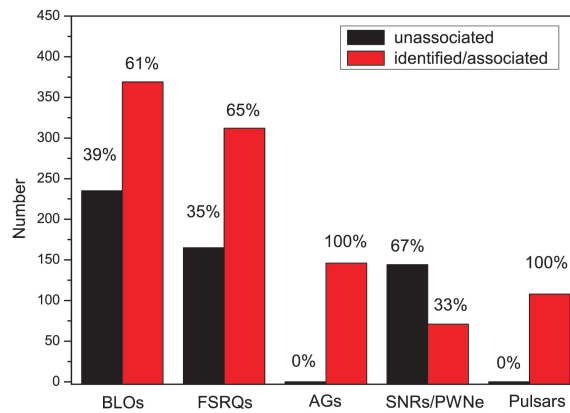
Fig. 7 The percentages of the unassociated and identified/associated sources classified as BLOs, FSRQs, AGs, SNRs/PWNe and pulsars, where the cosmological sources are only considered for $|b| \geq 18°$ in order to avoid complications due to the potential AGNs.

Firstly, the identification efficiencies of BLOs and FSRQs are comparable to each other, whereas the efficiency of SNRs/PWNs is much lower than the former two types. Such a situation could be understood as follows. On one hand, most BLOs and FSRQs can easily be distinguished from other types of sources by their characteristic rapid variability (large V). Moreover, the spectral energy distributions of BLO and FSRQ emission usually peak at two energy bands, i.e. the IR to X-ray band and the MeV to TeV band. The low-energy peak thus makes it relatively easy to find an IR (e.g. D'Abrusco et al. 2013; Massaro et al. 2013) or X-ray (e.g. ROMA-BZCAT sources; Massaro et al. 2009) counterpart. On the other hand, for SNRs, two types of gamma-ray emission scenarios have been widely investigated in literature, i.e. hadronic and leptonic scenarios (Blandford & Ostriker 1978; Becker et al. 2011; Schuppan et al. 2012). In the former case, gamma-ray emission is produced by neutral pion decay, whereas in the latter case it is by inverse-Compton scattering of relativistic electrons on some seed photons. It could be expected that, in the hadronic scenario, the low-energy emission is probably negligible unless there are some other emission regions. This makes it difficult to find low-energy counterparts for the gamma-ray SNRs. In other words, the low identification efficiency of SNRs may indicate that their gamma-ray emission is produced by hadrons. Very recently, Mandelartz & Becker Tjus (2013) indeed claimed that hadronic emission can be found in most Galactic SNRs. Future searches of TeV photons (e.g. by H.E.S.S.) could be helpful for distinguishing these two scenarios, because in the leptonic scenario the GeV and TeV photons have different origins.

Secondly, our statistical classification indicates that candidates of pulsars and AGs in unassociated sources must be very limited. In other words, the identification efficiencies of pulsars and AGs in the Fermi LAT catalog are close to unity, except for the GP region for AGs. Such high efficiencies could be due to (i) the plentiful multi-wavelength observations of AGs, which provide sufficient low-energy counterparts and (ii) the apparent gamma-ray pulsations of pulsars which significantly weakens the requirement of counterparts in other bands necessary for their identification.

4 CONCLUSIONS

According to their spatial distribution, 575 unassociated Fermi LAT sources can be separated empirically into GP, ISO and potential AGN components, the fractions of which are 25%, 55% and 20%, respectively. By comparing the spectral and variability properties of the different classes of unassociated sources with identified/associated sources, we conclude that the nature of the GP component is probably SNRs/PWNe, while the ISO component can further be separated into ISO-I and ISO-II subcomponents which are likely to be associated with BLOs and FSRQs, respectively. To be specific, the 575 unassociated sources could statistically consist of ∼144 SNRs/PWNe, ∼235 BLOs, ∼165 FSRQs and ∼31 AGs, where the constituents of the potential AGNs in the GP are considered to be the same as the identified/associated AGNs. The identification efficiencies of BLOs, FSRQs and SNRs/PWNe can further be estimated as 61%, 65% and 33%, respectively, except for the GP region where the efficiencies of BLOs and FSRQs become very low. By contrast, our result indicates that the identification efficiencies of pulsars and AGs could be very high. Anyway, the above conclusions are only viable statistically. The existence of some exotic sources cannot be ruled out, because we cannot individually determine the nature of the unassociated sources. Nevertheless, statistical classification may still be helpful for future identification or association of the sources.

References

Abdo, A. A., Ackermann, M., Ajello, M., et al. 2010, ApJS, 188, 405
Ackermann, M., Ajello, M., Allafort, A., et al. 2012, ApJ, 753, 83
Atwood, W. B., Abdo, A. A., Ackermann, M., et al. 2009, ApJ, 697, 1071
Becker, J. K., Black, J. H., Safarzadeh, M., & Schuppan, F. 2011, ApJ, 739, L43
Blandford, R. D., & Ostriker, J. P. 1978, ApJ, 221, L29
D'Abrusco, R., Massaro, F., Paggi, A., et al. 2013, arXiv: 1303.3002
Ferrara, E. C., Ojha, R., Monzani, M. E., & Omodei, N. 2012, arXiv: 1206.2571
Hartman, R. C., Bertsch, D. L., Bloom, S. D., et al. 1999, ApJS, 123, 79
Mandelartz, M., & Becker Tjus, J. 2013, arXiv:1301.2437
Massaro, E., Giommi, P., Leto, C., et al. 2009, A&A, 495, 691
Massaro, F., D'Abrusco, R., Paggi, A., et al. 2013, arXiv:1303.3585
Nolan, P. L., Abdo, A. A., Ackermann, M., et al. 2012, ApJS, 199, 31
Schuppan, F., Becker, J. K., Black, J. H., & Casanova, S. 2012, A&A, 541, A126
Stephen, J. B., Bassani, L., Landi, R., et al. 2010, MNRAS, 408, 422
Zechlin, H.-S., & Horns, D. 2012, J. Cosmol. Astropart. Phys., 11, 050